

# Physics 401 - Final Project

## The Ising Model

M. Ross Tagaras

*Department of Physics and Astronomy, Texas A&M University, College Station, TX 77845*

(Dated: October 29, 2019)

### INTRODUCTION

Theoretically describing magnetic systems provides a challenge. Not only are there myriad quantum effects, many-body calculations also have to be taken into account. It should therefore be nearly impossible to model any sort of magnetic system. However, the Ising model, first introduced in 1935, does an excellent job at reproducing many of the effects we see in such systems while performing only simple calculations. In this paper, we will use this model to examine the properties of the 2D ferromagnet, the 3D ferromagnet, and the 2D anti-ferromagnet. We will calculate magnetization, energy, susceptibility, and heat capacity. We will show that phase transitions exist for each system, and calculate the critical temperature for the 2D and 3D ferromagnets. Finally, we will calculate the critical exponents for these last two systems, which are used to classify the behavior of observables near the transition temperature.

### BACKGROUND

#### Statistical Mechanics

In the canonical ensemble, we can calculate the thermal average of some observable  $\mathcal{O}$ :

$$\langle \mathcal{O} \rangle = \frac{1}{Z} \int dr e^{-\beta H(r)} \mathcal{O}(r) \quad (1)$$

where the partition function  $Z$  is given by

$$Z = \int dr e^{-\beta H(r)} \quad (2)$$

We work in natural units, where Boltzmann's constant  $k_B = 1$ . In the discrete case, we can rewrite the thermal average as

$$\langle \mathcal{O}(x) \rangle = \frac{\sum_{i=1}^N e^{\beta H(x_i)} \mathcal{O}(x_i)}{\sum_{i=1}^N e^{\beta H(x_i)}} \quad (3)$$

To improve calculations done this way, we can modify this result via importance sampling[1] to get

$$\langle \mathcal{O}(x) \rangle = \frac{\sum_{i=1}^N e^{\beta H(x_i)} \mathcal{O}(x_i) / \mathbf{P}(x_i)}{\sum_{i=1}^N e^{\beta H(x_i)} / \mathbf{P}(x_i)} \quad (4)$$

where  $\mathbf{P}(x_i)$  gives the probability of a particular phase space configuration occurs. If we choose  $\mathbf{P}(x_i)$  to be the standard Boltzmann factor, then our expression reduces to the simple form

$$\langle \mathcal{O}(x) \rangle = \frac{1}{M} \sum_{i=1}^M \mathcal{O}(x) \quad (5)$$

### Specifics of the Ising Model

In Ising Model calculations, we construct a  $D$  dimensional lattice consisting of classical spins. Each site in this lattice has two states, up and down, which correspond to a value of  $+1$  and  $-1$  respectively. The sites interact with their nearest neighbors only.

The Ising Model Hamiltonian with no external field is given by[2]

$$H = - \sum_{\langle i,j \rangle} J_{ij} S_i S_j \quad (6)$$

where  $\sum_{\langle i,j \rangle}$  is a sum over nearest neighbors.  $S_i$  denotes the state of the  $i^{th}$  site and  $J_{ij}$  denotes the coupling between sites  $i$  and  $j$ .

The energy for a particular spin is given by [3]

$$\langle E \rangle = \left\langle \sum_{i=1}^N H_i \right\rangle = - \left\langle \sum_{i=1}^N \sum_{\langle ij \rangle} J_{ij} S_i S_j \right\rangle \quad (7)$$

where  $N = L^D$ . We can calculate  $\langle E^2 \rangle$  in a similar manner.

In this expression, we can see the importance of the sign of  $J_{ij}$ . If  $J_{ij} > 0$ , then to minimize the energy,  $S_i$  and  $S_j$  will tend to be aligned. If  $J_{ij} < 0$ , then the spins tend to take an opposite orientation. If we take  $J_{ij} = 1$  for all spins, then our system is ferromagnetic. If  $J_{ij} = -1$  for all spins, our system is anti-ferromagnetic. In a third case, we can randomly assign  $\pm 1$  to each interaction. This is known as a spin glass, but it is too computationally intensive to consider here.

We can also calculate the magnetization per spin, given by

$$M = \frac{1}{N} \sum_i S_i \quad (8)$$

$M^2$  and  $|M|$  are calculated similarly. From magnetization and energy, we can also calculate the heat capacity  $C$ , the susceptibility  $\chi$ , and  $g$ , the Binder cumulant[2]:

$$C = \frac{\partial E}{\partial T} = \frac{(\Delta E)^2}{T} = \frac{\langle E^2 \rangle - \langle E \rangle^2}{T} \quad (9)$$

$$\chi = \frac{\partial M}{\partial T} = \frac{(\Delta M)^2}{T} = \frac{\langle M^2 \rangle - \langle M \rangle^2}{T} \quad (10)$$

$$g = 1 - \frac{\langle m^4 \rangle}{3 \langle m^2 \rangle^2} \quad (11)$$

Not only are these quantities interesting in their own right, they will be useful when describing the phase transitions of our systems.

### The Metropolis Algorithm

Now that we have observables to calculate, we need a way to calculate them. For this, we use the Metropolis algorithm. The steps for this algorithm are[1]

1. Initialize the system at random
2. Choose a site at random
3. Compute a trial flip
4. Compute  $\Delta E = E_{trial} - E_{old}$ , the change in the energy of the system due to the trial flip
5. If  $\Delta E \leq 0$ , accept the new state and go to step 8
6. If  $\Delta E > 0$ , calculate  $e^{-\beta \Delta E}$
7. Generate a uniform random variable  $x$  in the interval  $[0,1]$
8. If  $x \leq e^{-\beta \Delta E}$ , accept the new state; otherwise retain the previous one
9. Calculate observables
10. Repeat until enough states have been obtained
11. Compute thermal averages

### Critical Exponents

Near a phase transition, the behavior of our observables can be characterized using critical exponents. We can describe a critical exponent for an arbitrary function:

$$\lambda = \lim_{t \rightarrow 0} \frac{\ln|f(t)|}{|t|} \quad (12)$$

which is equivalent to[3]

$$f(t) \sim |T - T_c|^\lambda \quad (13)$$

We will consider the critical exponents for heat capacity, magnetization, and susceptibility.

$$C \sim |T - T_c|^{-\alpha} \quad (14)$$

$$M \sim (T_c - T)^\beta \quad (15)$$

$$\chi \sim |T - T_c|^{-\gamma} \quad (16)$$

Furthermore, it can be shown[2] that these quantities are also related to the length of the lattice:

$$C \sim |T - T_c|^\alpha \rightarrow L^{\alpha/\nu} \quad (17)$$

$$M \sim (T - T_c)^\beta \rightarrow L^{-\beta/\nu} \quad (18)$$

$$\chi \sim |T - T_c|^\gamma \rightarrow L^{-\gamma/\nu} \quad (19)$$

From these relations, we can find the critical exponents for our systems, by doing calculations for several lattice sizes.

## THE TWO-DIMENSIONAL FERROMAGNET

First, we consider the simplest case - the 2D ferromagnet. In this case, we take  $J_{ij} = 1$  for all spins. We use a square lattice with side length  $L = 150$  and 5000 Monte Carlo sweeps per temperature. The temperature was lowered from  $T = 5$  to  $T = 0.05$  with  $dT = 0.005$ .

### Data and Results

First, we examine the magnetization of this system. To clearly see the change from disorder at high temperatures to order at low ones, it is more convenient to plot the absolute value of the magnetization. This helps to create the smooth curve shown below.

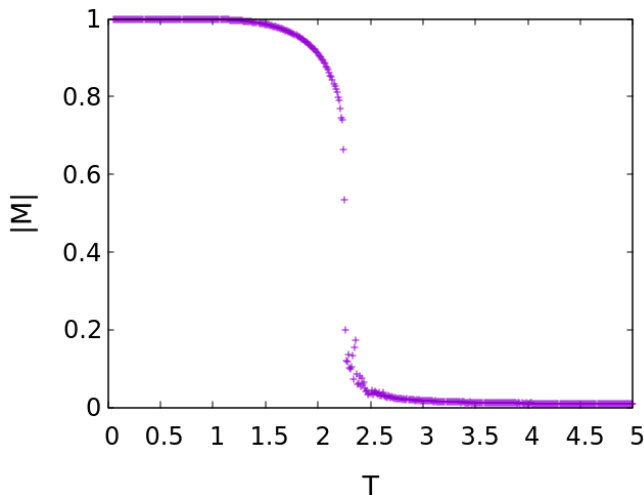


FIG. 1: Absolute value of magnetization vs. temperature for the 2D ferromagnet

As expected,  $|M|$  starts near zero, when all spins are randomly aligned. As the temperature is decreased, the value increases to 1.

Next, we plot the magnetic susceptibility  $\chi$ . The behavior here is mostly uninteresting, except in the region approximately between  $T = 2.2$  and  $T = 2.4$ , where we observe a sharp peak. This behavior will later be recognized as a sign of a phase transition.

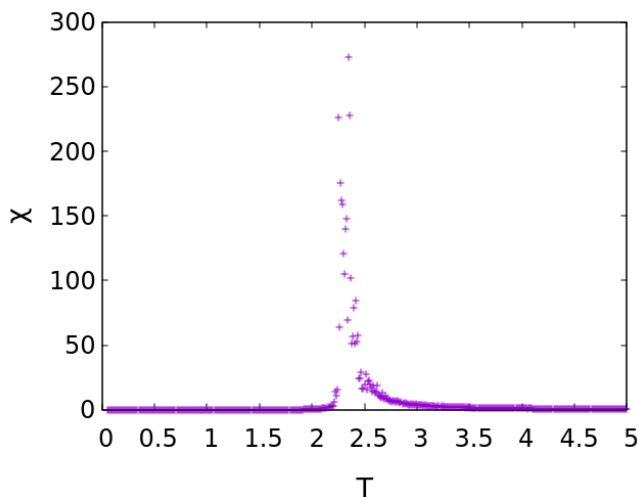


FIG. 2: Susceptibility vs. temperature for the 2D ferromagnet

We can also calculate the energy per spin. We notice that, as the magnet becomes ordered and the spins around any given point begin to take on the value at that point, the energy converges.

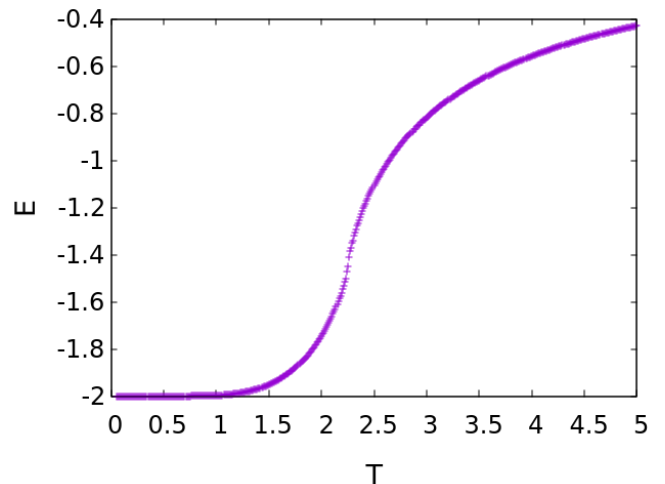


FIG. 3: Energy per spin vs. temperature for the 2D ferromagnet

Finally, we calculate the heat capacity. This tends to increase as we approach the region in which we are likely to find a phase transition, as expected.

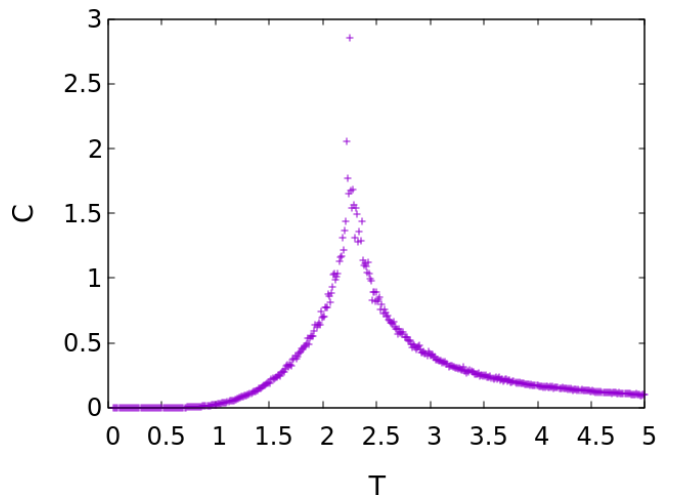


FIG. 4: Heat capacity vs. temperature for the 2D ferromagnet

### Qualitative Evidence for a Phase Transition

The simplest type of phase transition to find in our data is a  $2^{nd}$ -order one, where some observable has a singularity at the critical temperature. Due to the finite size of our lattice, there will not be a true divergence, but we can still examine the asymptotic behavior of our observables to find a region in which to look more closely with other methods. In this case, we see that the susceptibility begins to diverge somewhere around between  $T = 2.2$  and  $T = 2.4$ . We see similar but less dramatic behavior in the heat capacity in the same region. However, while this is a strong indication that a phase transition does

in fact occur, it does not help us determine the exact temperature at which a transition should take place. For that, we turn to the cumulant  $g$ .

### Calculation of the Critical Temperature

We can use the Binder cumulant to calculate the critical temperature. Since it is a dimensionless quantity, at the phase transition and once scaled to account for  $L$ , all  $g$  should be approximately equal[2]. This allows us a way to make a qualitative measurement of the phase transition previously observed. Here, we calculate  $g$  for lattice sizes  $L = 8, 16, 64$ . Since we need to make a very precise calculation, the number of Monte Carlo sweeps per temperature step was increased to 10,000. Even with this large number of sweeps, the behavior of  $g$  can be erratic, so we have performed a fit to improve our ability to cleanly find an intersection. This is plotted below.

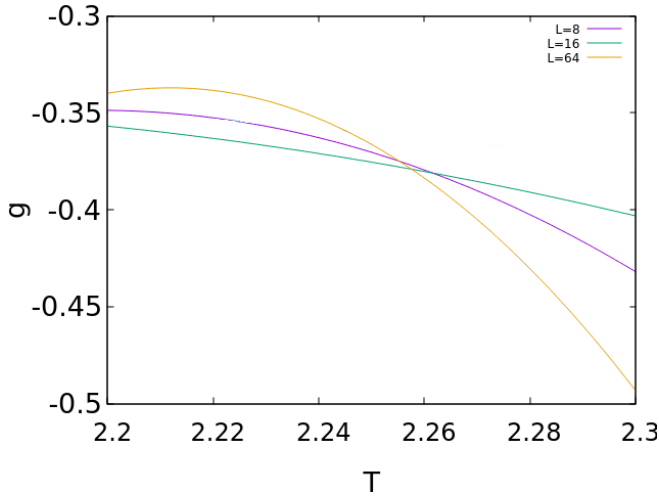


FIG. 5: Fittings for  $g$  for three lattice sizes

Taking the average of the very nearby intersections, we find a phase transition at  $T_c = 2.259$ .

### Calculating the Critical Exponents

Now that we have a value for  $T_c$ , we can proceed to find the critical exponents for our system. We have previously shown that, near  $T_c$ ,  $\chi$  obeys the relation

$$\chi \sim L^{\gamma/\nu} \quad (20)$$

where  $\nu = 1$  for the case of the two-dimensional Ising model[2]. Using the mean value[1] of  $\chi$  at  $T_c$ , this implies that

$$\ln \chi = \frac{1}{\gamma} \ln L \quad (21)$$

This relation is plotted below, for lattice sizes  $L = 8, 16, 32, 64$  with 5,000 Monte Carlo sweeps per temperature step.

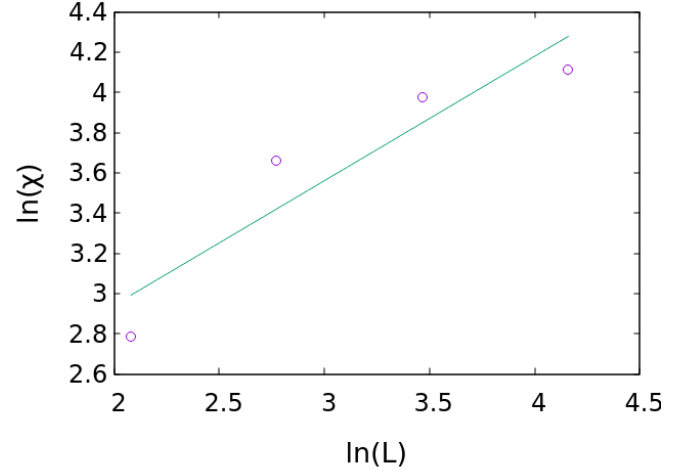


FIG. 6: Log plot of linear fitting of susceptibility vs.  $L$

We can perform a similar procedure for the magnetization:

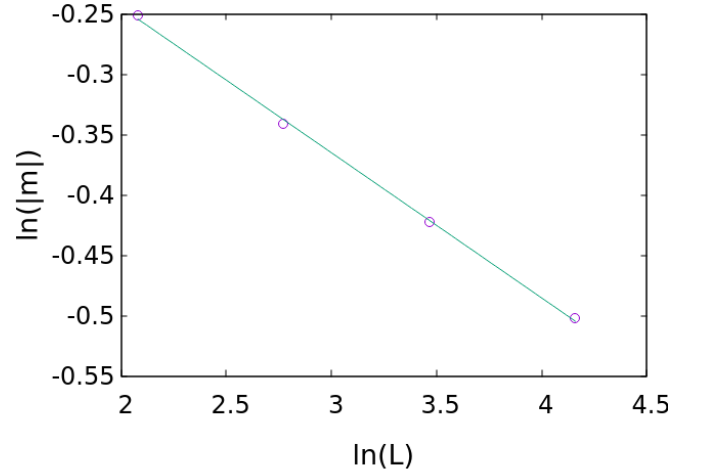


FIG. 7: Log plot of linear fitting of magnetization vs.  $L$

The case of the heat capacity is slightly more interesting. When plotted on log-scale axes, it is immediately apparent that this data can not be fit to linearly. As it turns out, the critical exponent[3] for  $C$  is  $\alpha = 0$ . With this in mind, we can instead plot the relation

$$C = C_0 \ln L \quad (22)$$

which is done below with  $L = 8, 16, 32$ . This is much more suited to a linear fit.

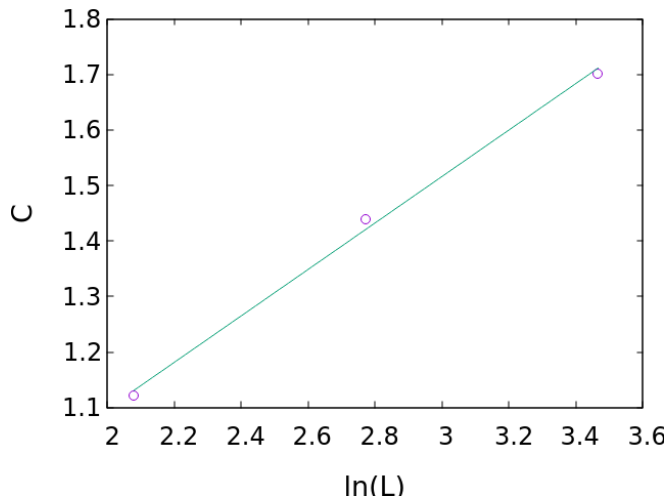


FIG. 8: Semilog fitting of heat capacity vs.  $L$ .

From these three fits, we find the critical exponents for this system to be

$$C_0 = .419 \pm .023 \quad (23)$$

$$\beta = .120 \pm .00236 \quad (24)$$

$$\gamma = 1.704 \pm .5569 \quad (25)$$

Notice that the uncertainty on these values is large. This is likely due to the small set of data points collected, the small lattice sizes used, and the difficulty in performing calculations with a small enough  $dT$  to result in good mean values for our observables while still spanning enough of the temperature range to ensure proper behavior near  $T_c$ .

### THE THREE-DIMENSIONAL FERROMAGNET

Now, we consider the three-dimensional case of the ferromagnet. In this case, we have a cubic lattice with side length  $L = 10$  and 2000 Monte Carlo sweeps per temperature step. The temperature was lowered from  $T = 15$  to  $T = 1$  with  $dT = .01$

#### Data and Results

The magnetization is essentially the same as in the 2D case. We notice that again, it converges to 1 as the temperature is decreased.

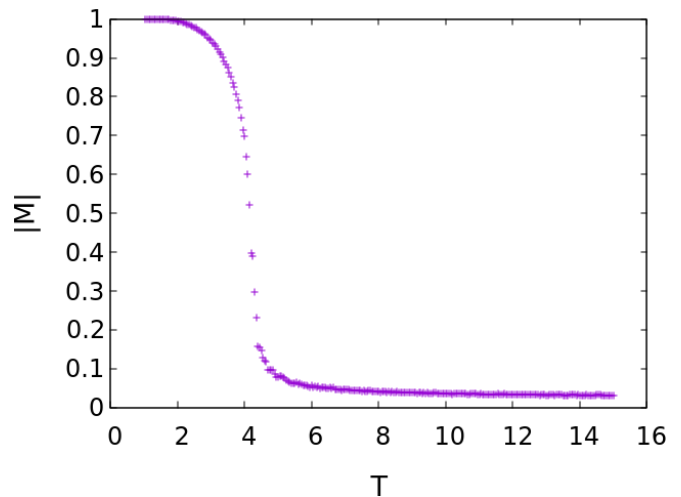


FIG. 9: Absolute value of magnetization vs. temperature for the 3D ferromagnet

The susceptibility has a similar form to  $\chi$  in the 2D case, but the peak has shifted.

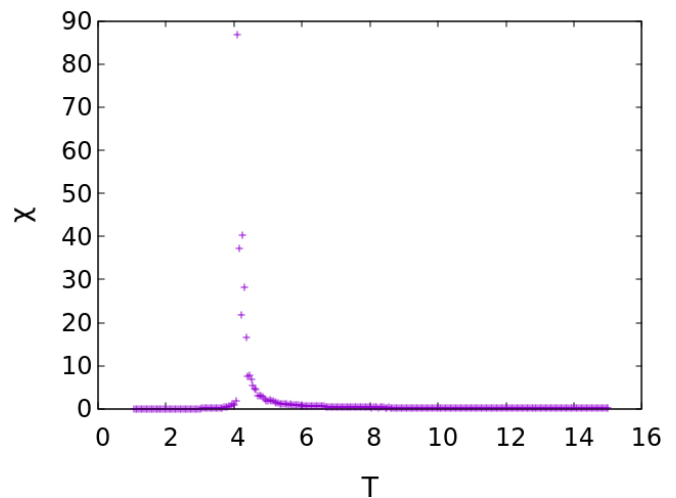


FIG. 10: Susceptibility vs. temperature for the 3D ferromagnet

Finally, the heat capacity has a similar form, but again is shifted. However, its peak is significantly sharper than the peak for the heat capacity of the 2D ferromagnet.

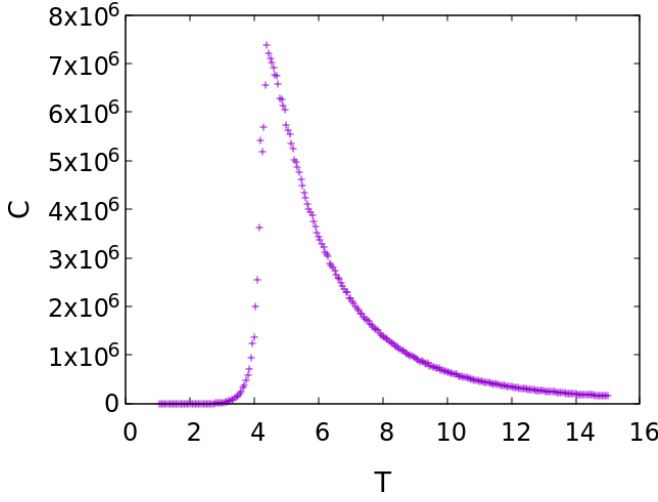


FIG. 11: Heat capacity vs. temperature for the 3D ferromagnet

### Qualitative Evidence for a Phase Transition

As before, we observe sharp peaks in the susceptibility and heat capacity. Both the shifts we observed in the last section indicate that the phase transition is no longer at the same temperature as in the 2D case, but is instead somewhere between  $T = 4$  and  $T = 5$ .

### Calculating the Critical Temperature

As before, to calculate  $T_c$ , we find fittings for  $g$  for lattice sizes  $L = 8, 10, 12$ .

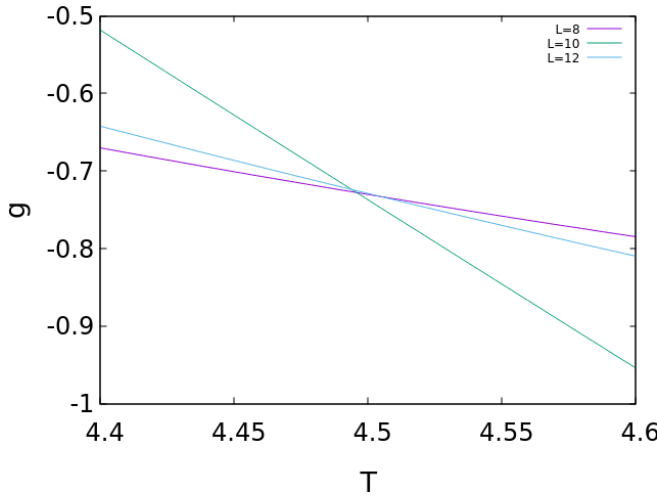


FIG. 12: Fittings for  $g$  for three lattice sizes

The average intersection point of the three fits is  $T_c = 4.50$ .

### Calculating the Critical Exponents

For the 3D ferromagnet, the value of  $\nu$  is known to be [5]  $\nu = .629971(4)$ . As before, we can calculate our critical exponents from the relations

$$C \sim L^{\alpha/\nu} \quad (26)$$

$$M \sim L^{-\beta/\nu} \quad (27)$$

$$\chi \sim L^{-\gamma/\nu} \quad (28)$$

In this case, the calculations were performed with lattice sizes of  $L = 6, 8, 10$ . The plots and fitting for these relations are shown below.

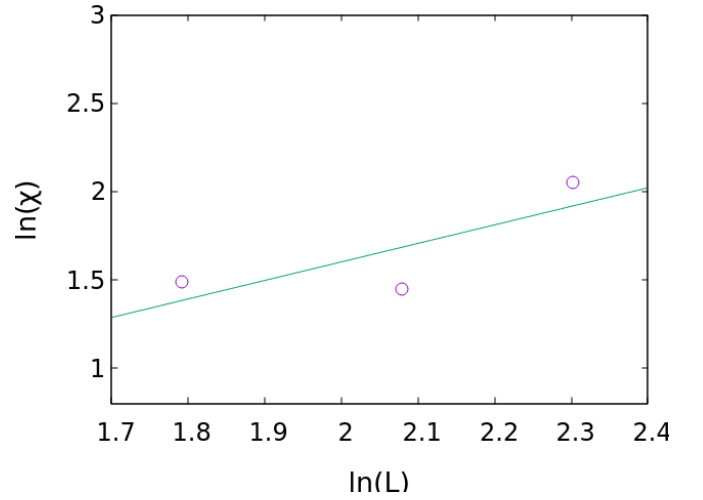


FIG. 13: Log plot of linear fitting of susceptibility vs.  $L$

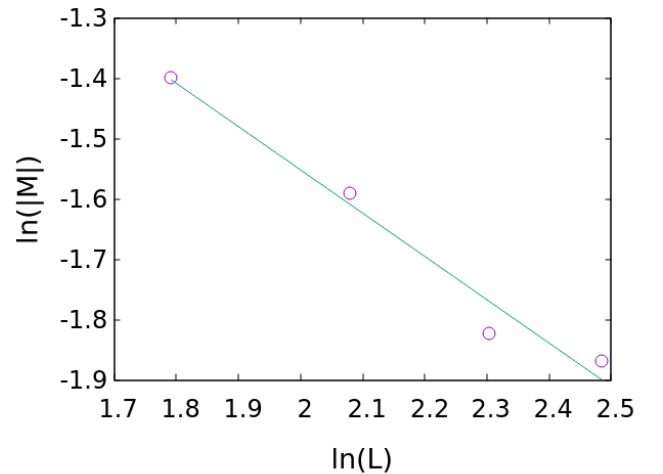


FIG. 14: Log plot of linear fitting of magnetization vs.  $L$

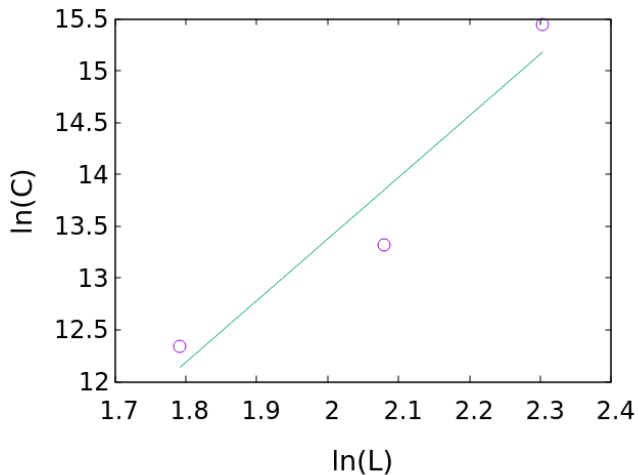


FIG. 15: Log plot of linear fitting of heat capacity vs.  $L$

From the fittings, we find that

$$\gamma = 1.67 \pm 0.8 \quad (29)$$

$$\beta = 0.44 \pm 0.08 \quad (30)$$

$$\alpha = .104 \pm .2 \quad (31)$$

Fortunately, in this case, we do not have the difficulty with fittings for  $\alpha$ . However, these values have substantial error. This is likely caused, as before, by the small lattice size and the lack of data points. Both these issues were ultimately caused by a lack of computing power.

## THE TWO-DIMENSIONAL ANTIFERROMAGNET

Finally, we turn to the anti-ferromagnetic counterpart to the 2D case we have just considered. Here, we take  $J_{ij} = -1$  for all spins. In general, these systems are more computationally intensive than their ferromagnetic counterparts, because of frustration effects that emerge because of each site's tendency to be different from its neighbors[4]. Because of this, we will not be able to calculate the exact  $T_c$  or the critical exponents. However, we can still show qualitative evidence for phase transitions and speculate that they are at the same  $T_c$  as in the ferromagnetic cases.

We use a side length of  $L = 150$  with 1000 Monte Carlo sweeps per temperature step. The temperature began at  $T = 15$  and was lowered to  $T = 0.5$  in steps of  $dT = 0.05$ .

### Data and Results

First, we calculate  $|M|$ . Notice that, unlike in the ferromagnetic case, this value tends to zero as  $T$  decreases.

This is expected, as the system should settle into an equilibrium with exactly half of the spins up, and half down.

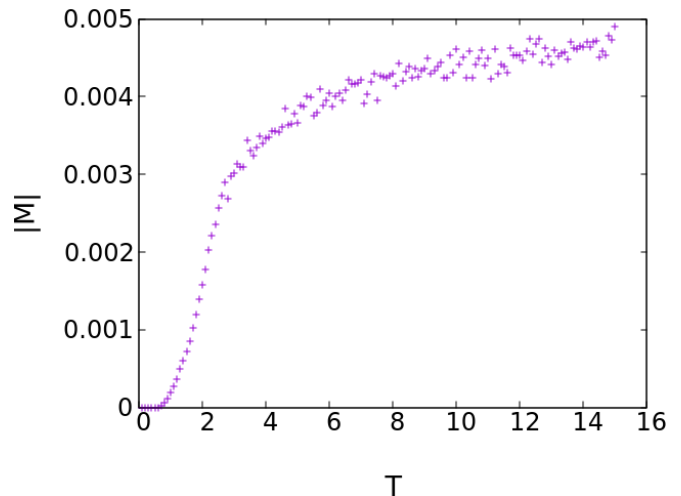


FIG. 16: Absolute value of magnetization vs. temperature for the 2D anti-ferromagnet.

The susceptibility is again different from the ferromagnet. It never forms a sharp peak, but instead has a kink at around  $T = 2.5$ . This is in fact the desired behavior[4].

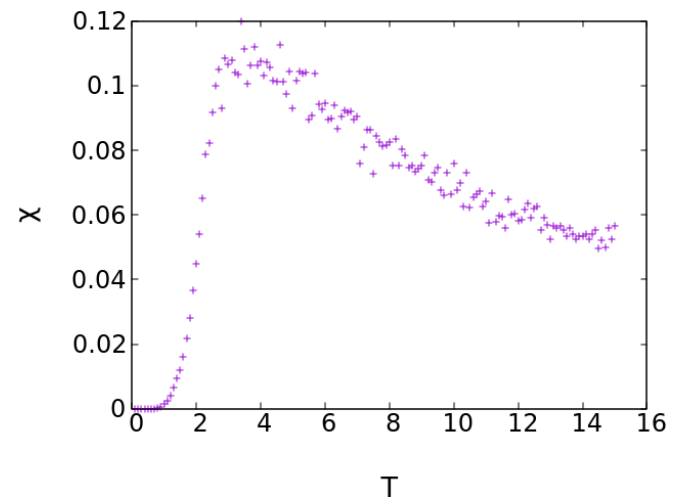


FIG. 17: Susceptibility vs. temperature for the 2D anti-ferromagnet

The energy per spin has essentially the same behavior as in the ferromagnet.

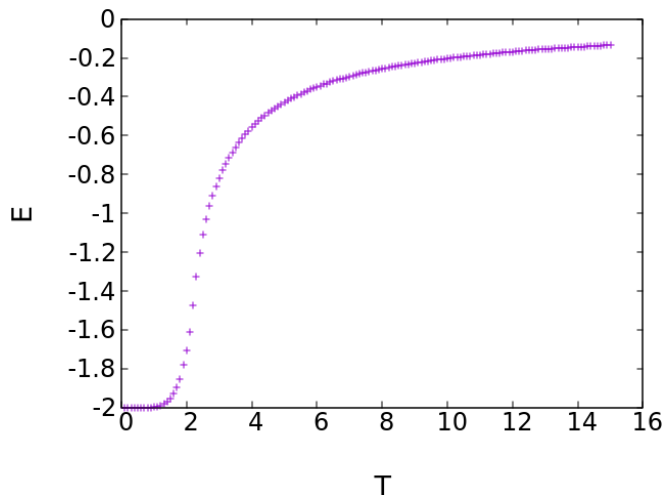


FIG. 18: Energy per spin vs. temperature for the 2D anti-ferromagnet

This is also the case for the heat capacity. The peak is not quite as sharp, but that is likely due to the increased computational difficulty of the problem.

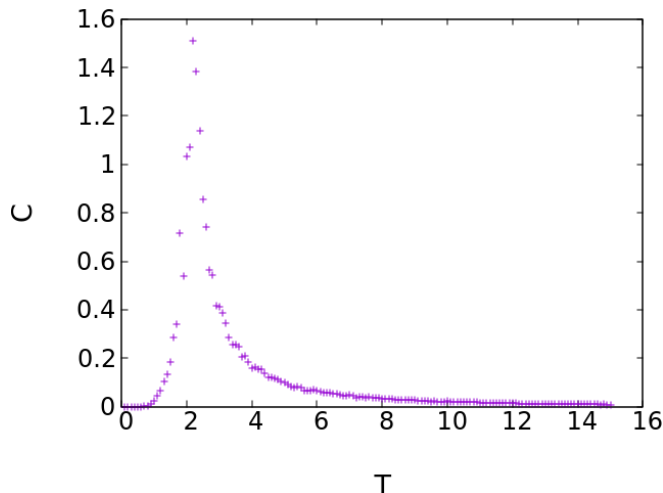


FIG. 19: Heat capacity vs. temperature for the 2D anti-ferromagnet

### Qualitative Evidence for a Phase Transition

We notice that the peak in the heat capacity as well as the kink in the susceptibility both occur in a very similar range to the ferromagnetic case. It is likely that the  $T_c$  is the same for the ferromagnet and the anti-ferromagnet. As it turns out, this is the case[1].

### CONCLUSIONS

Using the Metropolis algorithm, we were able to calculate magnetization, susceptibility, energy, heat capacity,

and the Binder cumulant for the 2D ferromagnet, the 3D ferromagnet, and the 2D anti-ferromagnet. From this information, we were able to calculate the critical temperature for the 2D and 3D ferromagnets, as well as their critical exponents corresponding to magnetization, susceptibility, and heat capacity. The data we obtained above is reproduced below for easy referencing, along with the commonly accepted values[3][5] for these quantities.

Quantity	Value	Accepted Value
$T_c$ (2D ferromagnet)	2.259	2.269
$C_0$	$0.419 \pm 0.023$	0.5
$\beta$	$0.120 \pm .00236$	0.125
$\gamma$	$1.701 \pm .5569$	1.75
$T_c$ (3D ferromagnet)	4.50	4.512
$\alpha$	$0.104 \pm 0.2$	0.11008
$\beta$	$0.44 \pm 0.08$	0.326419
$\gamma$	$1.67 \pm 0.8$	1.237075

TABLE I: Comparison of calculated values to accepted values

As we see from the above table, the accepted values for the quantities we have calculated are typically within our uncertainty.

We also obtained qualitative evidence that the critical temperature is the same for both the 2D ferromagnet and the 2D anti-ferromagnet.

With more computing power, it would have been possible to calculate the exact  $T_c$  for the 2D anti-ferromagnet, as well as its critical exponents. It would also have been possible to make these measurements for the 3D case.

The basic techniques used here can also be applied to the Ising spin glass, where  $J_{ij}$  is randomly assigned to each site, instead of being constant. The procedure for solving these systems is much more complex, and typically requires algorithms more advanced than the implementation of the Metropolis algorithm used here.

- 
- [1] H. Gould, J. Tobochnik, W. Christian. "An Introduction to Computer Simulation Methods" (2016)
  - [2] H. Katzgraber. "Introduction to Monte Carlo Methods". arXiv:0905.1629v3 [cond-mat.stat-mech], 2011.
  - [3] J. Kotze. "Introduction to Monte Carlo methods for an Ising Model of a Ferromagnet". arXiv:0803.0217v1 [cond-mat.stat-mech], 2008.
  - [4] M. Fisher, M. Sykes. "Antiferromagnetic Susceptibilities of the Simple Cubic and Body-Centered Ising Lattices". *Physica*, 28, 1962
  - [5] E. Sheer, M. Paulos, D. Poland, S. Rychkov, D. Simmons-Duffin, A. Vichi. "Solving the 3d Ising Model with the Conformal Bootstrap II. c-Minimization and Precise Critical Exponents". *Journal of Statistical Physics*. 157 (2014)